Available online at www.sciencedirect.com
SCIENCE DIRECT®
PERGAMON
International Journal of Heat and Mass Transfer 46 (2003) 3737–3746
International Journal of HEAT and MASS TRANSFER
www.elsevier.com/locate/ijhmt

Heat transfer characteristics of spray cooling in a closed loop

Lanchao Lin [a,*], Rengasamy Ponnappan [b]

[a] Universal Energy Systems, Inc., 4401 Dayton-Xenia Road, Dayton, OH 45432-1894, USA
[b] Air Force Research Laboratory, Propulsion Directorate, Wright-Patterson AFB, OH 45433-7251, USA

Received 13 December 2002; received in revised form 11 April 2003

Abstract

A closed loop spray cooling test setup is established for the cooling of high heat flux heat sources. Eight miniature nozzles in a multi-nozzle plate are used to generate a spray array targeting at a 1×2 cm^2 cooling surface. FC-87, FC-72, methanol and water are used as the working fluids. Thermal performance data for the multi-nozzle spray cooling in the confined and closed system are obtained at various operating temperatures, nozzle pressure drops (from 0.69 to 3.10 bar) and heat fluxes. It is exhibited that the spray cooler can reach the critical heat fluxes up to 90 W/cm^2 with fluorocarbon fluids and 490 W/cm^2 with methanol. For water, the critical heat flux is higher than 500 W/cm^2. Air purposely introduced in the spray cooling system with FC-72 fluid has a significant influence on heat transfer characteristics of the spray over the cooling surface.

Keywords: Spray cooling; Heat transfer enhancement; Nucleate boiling heat transfer; Two-phase flow

1. Introduction

Spray cooling as the high heat flux removal technique has potentials for high power systems. The spray cooling with phase change takes advantage of relatively large amounts of latent heat and is capable of removing high heat fluxes from surfaces with low superheat. With water as the working fluid, a spray cooling heat flux of 1000 W/cm^2 has been demonstrated [1]. Recent applications of spray cooling involved the cooling of different kinds of electronics. In the application, a major portion of heat transfer results from nucleate boiling heat transfer. Other emerging applications include the cooling of high power directed energy sources operating in the space environment and generating heat at heat flux levels greater than 500 W/cm^2.

Several experiments were performed by many researchers in order to understand nucleate boiling heat transfer and critical heat flux (CHF) for full cone sprays using single nozzles [1–6] and multiple nozzles [7]. The effects of spray nozzle, volumetric flux, Sauter mean diameter (SMD) of spray, subcooling and working fluid were investigated. The heat transfer mechanism of spray cooling is associated with phenomena such as nucleate boiling due to both surface nucleation and secondary nucleation, convection heat transfer, and direct evaporation from the surface of liquid film [2]. The concept of secondary nucleation is helpful for understanding the heat transfer enhancement of spray cooling. It has been concluded that increasing the droplet flux increases the number of secondary nuclei, increases heat transfer of nucleate boiling and convection, and helps to lower surface temperature for a given heat flux [2].

Mudawar and Valentine conducted an experimental study of spray cooling to determine local quenching characteristics for various regimes of a water spray boiling curve [3]. It was found that the volumetric flux had a dominant effect on heat transfer compared to other hydrodynamic properties of the spray [3]. Sehmbey et al. investigated the effect of surface material properties and surface characteristics on spray cooling heat transfer using air atomized nozzles [4]. A higher contact angle showed an enhanced heat transfer due to

* Corresponding author. Tel.: +1-937-255-3092; fax: +1-937-904-7114.
E-mail address: lanchao.lin@afrl.af.mil (L. Lin).

0017-9310/03/$ - see front matter © 2003 Elsevier Ltd. All rights reserved.
doi:10.1016/S0017-9310(03)00217-5

Nomenclature

c_w	constant
d_o	nozzle orifice diameter, m
d_{32}	Sauter mean diameter, m
h_{fg}	latent heat of vaporization, J/kg
h	heat transfer coefficient, W/m^2 K
k_h	thermal conductivity of heater plate, W/m K
p_1	pressure at the outlet of condenser, Pa
p_2	pressure at the inlet of liquid chamber, Pa
p_3	spray chamber pressure, Pa
q''	heat flux (heat rate per unit cooling area), W/cm^2
q''_c	critical heat flux, W/cm^2
Q''	volumetric flow rate per unit cooling area, m^3/m^2 s
t_1	distance between the hot surface and nearer thermocouple plane in the heater plate, m
t_2	distance between two thermocouple location planes, m
T	temperature, °C
T_b	boiling point, °C
T_{ch}	spray chamber temperature, °C
$T_{ch,o}$	spray chamber outlet temperature, °C
Δp	pressure drop across spray nozzle, Pa
η_c	effectiveness of spray cooling at CHF
μ_l	liquid dynamic viscosity, N s/m^2
ρ	density, kg/m^3
σ	surface tension, N/m

Subscripts

l	liquid
m	mean value
sat	saturation
v	vapor
w	cooling surface

the ease in nucleation and a smooth surface (0.3 μm polish) showed a dramatic increase in heat flux due to the thinner liquid film [4]. Yang et al. presented a heat transfer correlation based on water spray data in the nucleate boiling regime [1]. In their experiment, an air atomized nozzle was used. Estes and Mudawar presented a CHF correlation with suitable dimensionless parameters that accurately predicted data for FC-72, FC-87 and water [5]. The correlation by Estes and Mudawar had a strong dependence of CHF on volumetric flux and Sauter mean diameter. Sehmbey et al. developed a semiempirical correlation for CHF that was based on macro-layer dryout model and correlated with data for water and LN2 [6]. Lin and Ponnappan investigated CHF of multi-nozzle spray cooling in a closed loop and obtained a CHF correlation using their experimental data [7].

Most available spray cooling data were related with the free spray cooling in a large space or the spray cooling of small surfaces using single nozzle. In most experiments, the applied pressure drops across the nozzle were greater than 2.0 bar [3–6] and there existed air, more or less, in the spray cooling systems [1–6]. The present investigation deals with multi-nozzle spray cooling in the confined spray chamber and the flow is circulated within a closed loop. The test setup is established to simulate the cooling of high power laser diode arrays (LDAs). The use of spray cooling technology in this application is to ensure a minimum temperature gradient between emitters and along the cavity length of the emitter. A multi-nozzle plate embedded with eight miniature nozzles is used. The target spray cooling area is 1×2 cm^2 and the design is scaleable to large cooling areas for LDA application. The applied pressure drops across the nozzle range from 0.69 to 3.1 bar. To maintain the optimum thermal performance of the closed loop spray cooling system, the system is evacuated before filling a proper amount of the working fluid. Heat transfer characteristics of the closed loop spray cooling system are presented. The effect of the noncondensible gas on the thermal performance of the spray cooling is described.

2. Test setup and procedure

2.1. Multi-nozzle assembly

A hot surface area of 1×2 cm^2 is designed for the spray cooling test. To generate a spray array impinging on the cooling surface, eight miniature nozzles are made in a multi-nozzle plate as shown in Fig. 1. Each nozzle has a swirler insert of 3.18 mm in diameter and 1.0 mm thick as shown in Fig. 2. The swirler insert is mounted onto the multi-nozzle plate. There are three swirl ports and one center port with a diameter of 0.2 mm in the swirler insert. The liquid jet entering the center port interacts with the jets from the swirl ports and this generates a swirl flow pattern in the swirl chamber with an inner cone angle of 60°. The swirling liquid jet coming out from the discharge orifice causes a wide spray angle and intensifies liquid breakup into fine droplets. The nozzle discharge orifice below the conical swirl chamber is a 0.15 mm long through-hole with a

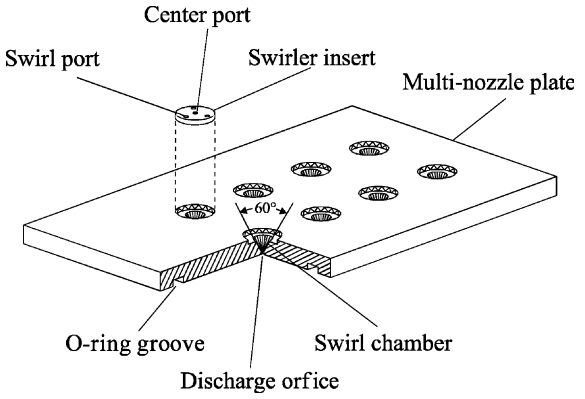

Fig. 1. Multi-nozzle assembly.

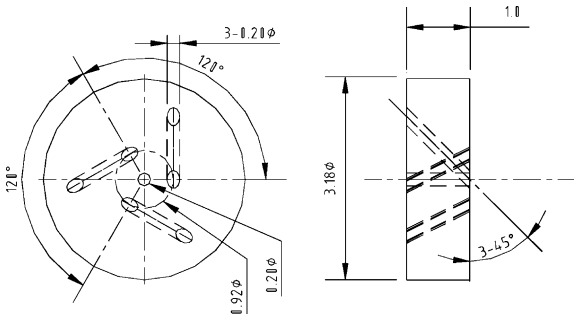

Fig. 2. Swirler insert (dimensions in mm).

diameter of 0.25 mm. The distance between two nozzles is 5.0 mm.

Performance tests of the nozzle array using FC-72, FC-87 and water in the atmospheric environment exhibited that the nozzles are capable of generating full cone spray patterns with spray cone angles larger than 35° at spray pressure drops greater than 1.72 bar. In the case of FC-72 spray at $\Delta p = 2.76$ bar, an average spray cone angle of 50° is obtained.

2.2. Thermal performance experiment

The test setup is designed for the measurement of CHF and the thermal performance of the multi-nozzle spray cooling. The schematic of test setup is shown in Fig. 3. The system consists of the multi-nozzle plate, a heater assembly, a liquid chamber, a spray chamber, a helical coil condenser, flow channels (for two-phase flow and liquid flow), a magnetic gear pump, a preheater, a bypass loop, and a filter. A cold bath is used to supply cooling water to and from the condenser. The spray chamber is connected with the heater plate which is on the top of the heater block (heat focusing block). The cooling surface of the heater plate is polished with 14 μm grit SiC paper before testing. The distance between the nozzle exit and the cooling surface is 8.8 mm which is sufficiently high for breaking up the liquid into fine droplets. The spray chamber space dimensions are 8.8 mm (high), 28.5 mm (long) and 17.0 mm (wide).

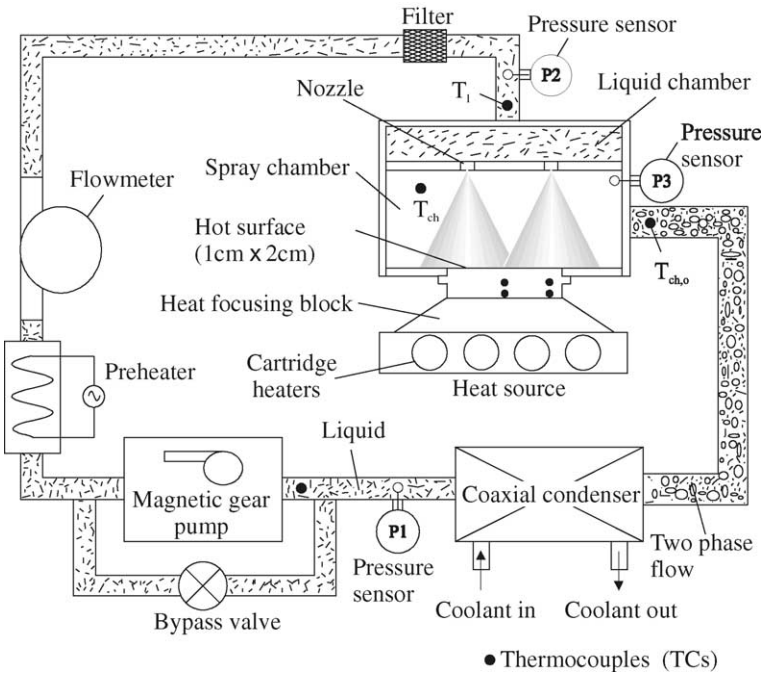

Fig. 3. Schematic of experimental setup.

Working fluids include FC-87, FC-72, methanol and water. The system of the closed loop is evacuated to a pressure below 5×10^{-6} Torr before filled with the working fluid. The liquid fill amount is 190 ml which is about 38% of the internal volume of the loop. The pressure difference generated by the micro-pump maintains the circulation flow. The multiple sprays interfere with adjacent ones in the near surface region. The liquid with an elevated pressure is accumulated in the liquid chamber before ejecting through the nozzles so that each nozzle will approximately contribute the same momentum to the spray chamber. In the spray chamber, the slightly subcooled droplets impinge onto the hot surface. A large part of the droplets turn into a thin film on the hot surface and a small part of them vaporize, removing the heat through phase change. The vapor flows along with the liquid out of the spray chamber into the two-phase channel which guides the two-phase flow to the condenser where the vapor condenses. The subcooled liquid from the condenser is pumped back to the liquid chamber. The spray cooling capability is limited by CHF from the hot surface.

The liquid flow rate of the spray cooling system is measured using a turbine flow meter operating with a signal conditioner. The spray chamber pressure (p_3), the pressure at the inlet of the liquid chamber (p_2) and the pressure at the outlet of the condenser (p_1) are measured using three pressure sensors. The spray chamber pressure corresponds to the fluid saturation temperature, T_{sat}, in the spray chamber. The spray pressure drop, the pressure difference between the supply pressure (p_2) and spray chamber pressure (p_3), is controlled by the pump and bypass valve. The rotational speed of the magnetic pump is adjustable through a DC power supply. The working fluid temperatures at the four locations in the spray cooling loop are measured using T-type probe thermocouples as shown in Fig. 3. The supply liquid temperature (at the inlet of liquid chamber), T_l, is regulated by adjusting the cold bath temperature and input power to the preheater. It is desired that T_l is set to be as close to T_{sat} as possible to minimize the subcooling effect.

A heater block made of copper with four cartridge heaters is used as the heat source. The heater plate with the hot surface towards the spray chamber is embraced by an insulation plate made of silicone and glass, G7, and is tightly attached to the heater block by a compression assembly. Thermal grease is used to minimize the contact thermal resistance between the heater plate and heater block. Eight thermocouples are embedded in 0.58 mm holes drilled along two planes in the heater plate, forming four pairs of thermocouples. Four thermocouple locations in the front of the heater plate are shown in Fig. 3. The distance between two thermocouple location planes, t_2, is 2.54 mm. The distance between the cooling surface and the upper plane of the thermocouple locations, t_1, is 2.16 mm. The thermocouple bead diameter is 0.3 mm. The heater assembly is well insulated with fiberfrax. The hot surface heat flux is calculated by

$$q'' = \frac{c_w k_h}{t_2}(T_{2,m} - T_{1,m}), \tag{1}$$

where $T_{1,m}$ and $T_{2,m}$ are the arithmetic means of the temperatures indicated by the four thermocouples at the upper plane and those at the lower plane, and the constant c_w is obtained through calibration (described in Section 3). The average temperature on the hot surface, T_w, is calculated by

$$T_w = T_{1,m} - \frac{q''t_1}{k_h}. \tag{2}$$

AC power is applied to the cartridge heaters. The AC voltage is adjustable through a variac. The input power is monitored by a power analyzer (MAGTROL).

All signals of the measured parameters are transferred to PC for recording. During the test, the input power is varied from 20 to 1020 W or up to the amount relating with CHF. The spray pressure drop is adjusted at the levels of 0.69, 1.03, 1.72, 2.41 and 3.1 bar. The spray chamber pressure is varied according to the working fluid being used. All data are acquired 50 times in an interval of 1 min and the average values are recorded after a steady state is reached.

To observe the spray pattern in the spray chamber, the frame of the spray chamber is replaced with a transparent material (acrylic material) with the same dimensions as the metallic frame used for the performance test. FC-72 is used as working fluid. During visual observation, operating conditions such as the pressure drop, input power and spray chamber temperature are varied.

3. Measurement uncertainty

A data acquisition system is used to record all temperature measurements. This device has a resolution of 0.02 °C. The data acquisition unit and T-type thermocouples are compared to a precision digital resistance temperature device with 0.03 °C rated accuracy. The system accuracy is found to be within 0.2 °C over the range of interest. In the steady state, the thermocouples fluctuate within 0.2 °C.

The uncertainty of the electrical power through the power analyzer is 0.5% of reading. The accuracy of the distance between two thermocouples in each pair in the heater plate is 0.1 mm and the accuracy of the distance between the cooling surface and the upper level of the thermocouple locations in the heater plate is 0.15 mm. The uncertainty of the cooling surface area of the heater plate is 0.05 cm^2. To reach a lower uncertainty of the heat flux measurement, the effective distance

between the upper level and lower level of the thermocouple locations is calibrated by measuring heat losses of the heater block and plate. To do this, the heater block and plate are covered with an insulation material and a small electric power load is applied to the cartridge heater. The applied electric power load is adjusted until a specific temperature of the heater block is reached. During the measurement, the heater block temperature is varied. The heat loss is 15 W at the heater block temperature of 250 °C. The actual heat rate through the cooling surface is estimated by subtracting the heat losses from the input power. The actual heat rate and the measured temperatures in the heater plate for the same input power are used to determine the effective distance of the thermocouple locations. The uncertainty of the heat flux is 4.8% at $q'' = 50$ W/cm^2 which is the smallest CHF data obtained in the present experiment. In this case the uncertainty of T_w is estimated within 0.33 °C. At $q'' = 490$ W/cm^2, the uncertainty of T_w is estimated within 2.1 °C. It is noted that the effect of the temperature gradient across the thermocouple beads in the heater plate is not considered in the uncertainty analysis.

The accuracies of the pressure sensors at the inlet of liquid chamber, at the outlet of condenser and in the spray chamber are 6.0×10^{-3}, 2.6×10^{-3} and 8.6×10^{-3} bar. The saturation temperature, T_{sat}, is calculated as function of the spray chamber pressure. The uncertainty of T_{sat} is estimated within 0.3 °C. The turbine flow meter is calibrated for FC-72, and water. The uncertainty of the flow rate is 3% of reading. The uncertainty of Q'' is estimated to be 3.9%.

4. Results and discussion

4.1. Spray cooling pattern

It is observed in the visualization experiment that nucleate boiling heat transfer occurs in all tested cases. The spray cones are surrounded by the agitated two-phase fluid. A schematic of a typical spray cooling pattern in the spray chamber is shown in Fig. 4. The droplets impinge onto the hot surface and splash to the side. The splashing liquid is restricted by the wall and forced to rebound to the space surrounding the sprays. It is conceivable that the interaction between the spray cone and surrounding fluid is stronger in the case of multi-nozzle spray cooling than in the case of single nozzle spray cooling.

4.2. Heat transfer characteristics

Experimental data expressing heat transfer characteristics, q'' vs. $T_w - T_{sat}$, for FC-87, FC-72, water and methanol are presented in Fig. 5–11. The values of the volumetric flux, Q'', or the nozzle pressure drop, $\Delta p = p_2 - p_3$, refer to the conditions pertinent to the curves. The volumetric flux is defined as the total liquid volumetric flow rate divided by the hot surface area. Also presented in these figures are the different saturation temperatures, T_{sat}, in the spray chamber and the subcooling, $T_{sat} - T_l$, where T_l is the liquid temperatures. Fig. 5 shows the effect of volumetric flux on heat transfer characteristics for FC-87 at $T_{sat} = 42$ °C. Figs. 6 and 7 give the data for FC-72 at $T_{sat} = 53$ and 36 °C. The values of subcooling, $T_{sat} - T_l$, are very small for these cases. Generally, the surface superheat, $T_w - T_{sat}$, increases with an increase of the heat flux, q''. For a given surface superheat, the heat flux increases with the volumetric flux. As seen from the figures, the slope of the curves varies with the superheat. In the lower superheat region, e.g., $T_w - T_{sat} < 15$ °C, the slope of the curves is relatively small and does not change much. In this case,

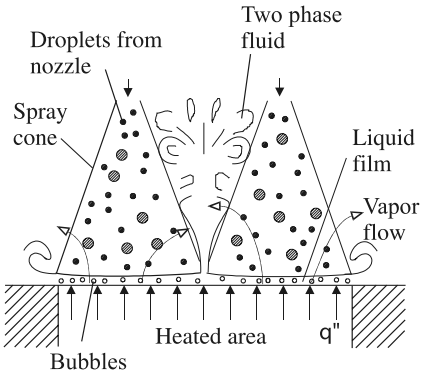

Fig. 4. Spray cooling pattern.

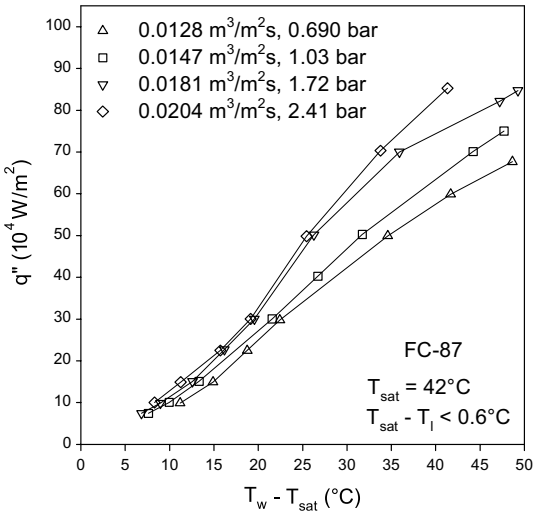

Fig. 5. Effect of volumetric flux on heat transfer characteristics for FC-87 at $T_{sat} = 42$ °C.

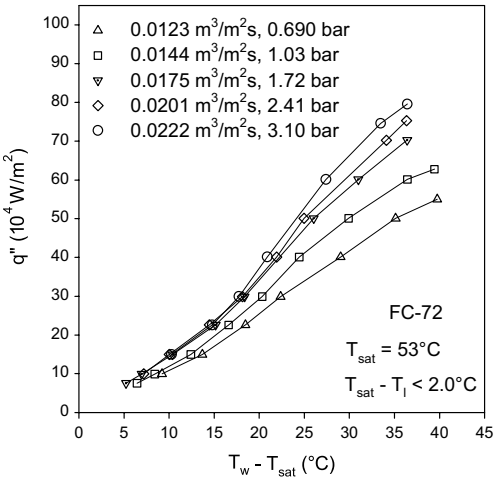

Fig. 6. Effect of volumetric flux on heat transfer characteristics for FC-72 at $T_{sat} = 53$ °C.

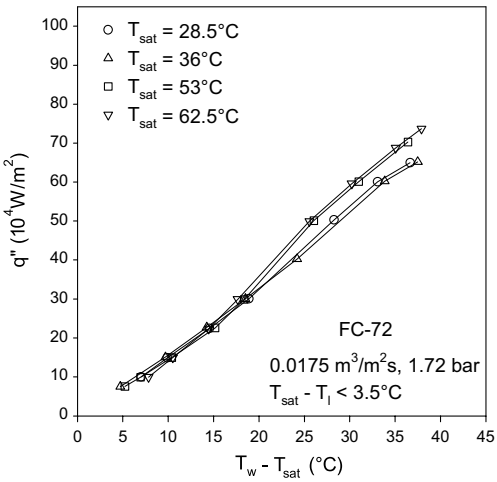

Fig. 8. Effect of spray saturation temperature on heat transfer characteristics for FC-72 at $\Delta p = 1.72$ bar.

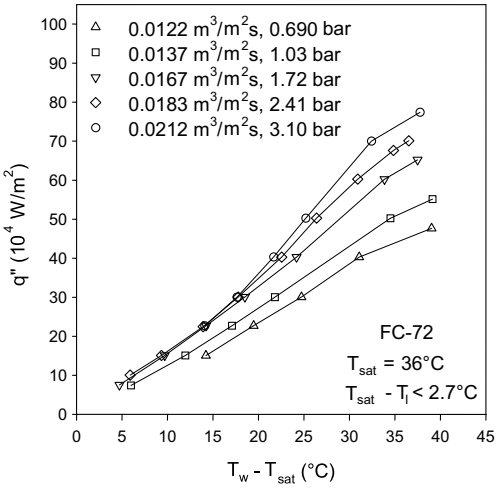

Fig. 7. Effect of volumetric flux on heat transfer characteristics for FC-72 at $T_{sat} = 36$ °C.

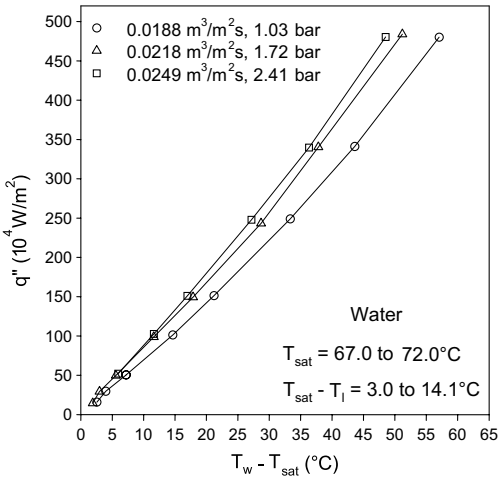

Fig. 9. Effect of volumetric flux on heat transfer characteristics for water at $T_{sat} = 67$–72 °C.

the heat transfer is mainly ruled by convection along with evaporation from the surface of liquid film though slight nucleate boiling is existing. As the surface superheat exceeds a point, around 15 °C, the slope of the curves increases and then turns to decreasing. This trend indicates that the nucleate boiling heat transfer is becoming a major part of heat transfer and then the transport process involves more convection and evaporation of the liquid film until dryout occurs. At pressure drops above 1.72 bar or volumetric fluxes greater than 0.017 m^3/m^2 s, the increase in heat flux due to an increase of the pressure drop becomes small. This is due to the fact that a higher volumetric flux results in a thicker liquid film that decreases the evaporation from the free surface, thus partially counteracts the effect of increased convection. This also implies that the pressure drop of 1.72 bar or lower may not be optimum for the maximum heat removal.

Fig. 8 shows the effect of spray saturation temperature on heat transfer characteristics for FC-72 at $\Delta p = 1.72$ bar. The subcooling is smaller than 3.5 °C. It can be seen that the change in the relation of q'' with $T_w - T_{sat}$ is small as the saturation temperature is varied. This is because the nucleation sites at the hot surface do not change much at the same volumetric flux. It is noted that the variation of the sprayed surface temperature is within 1.5 °C for the fluorocarbon fluids (FC-87 and FC-72).

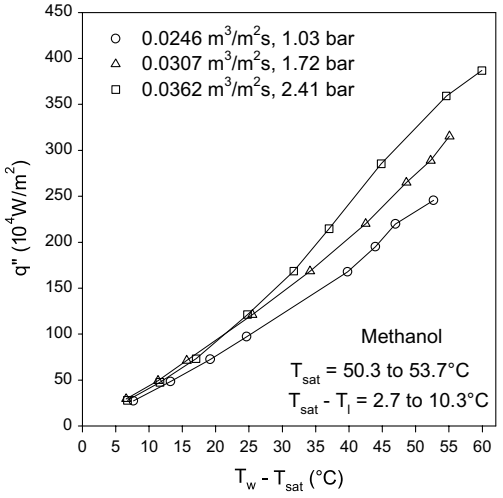

Fig. 10. Effect of volumetric flux on heat transfer characteristics for methanol at $T_{sat} = 50.3$–53.7 °C.

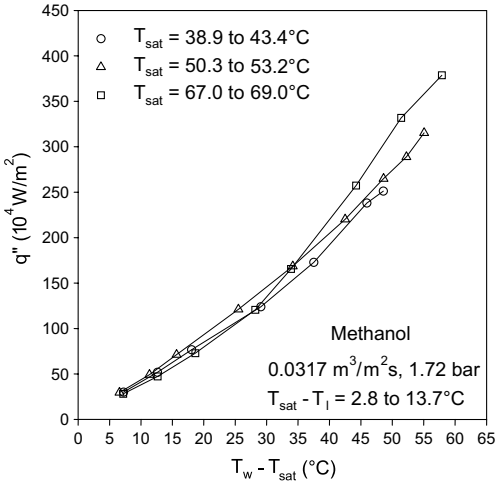

Fig. 11. Effect of spray saturation temperature on heat transfer characteristics for methanol at $\Delta p = 1.72$ bar.

Fig. 9 shows the effect of volumetric flux on heat transfer characteristics for water at $T_{sat} = 67$–72 °C. The subcooling for water (between 3.0 and 14.1 °C) is higher than the cases of fluorocarbon fluids but is still considered as being small since CHF for water is much higher. The surface superheat increases with an increase of the heat flux. The change in the slope of the curves is small with a variation of the superheat. It seems similar to the cases of fluorocarbon fluids that the pressure drop greater than 1.72 bar is required to reach high heat fluxes. Since the maximum input power is 1020 W, the data points exceeding 500 W/cm^2 are not obtained for water.

Figs. 10 and 11 show the heat transfer characteristics using methanol as the working fluid. The subcooling for methanol (between 2.7 and 13.7 °C) is still small since CHF for methanol is much higher. The relation of the heat flux with the superheat, as shown in Fig. 10, is somewhat like the cases of fluorocarbon fluids but the achievable heat fluxes are much higher than those for FC-87 and FC-72. The variation of the slope of the curves in Fig. 10 reveals that the boiling heat transfer becomes more important at the superheats greater than 30 °C. As seen from Fig. 11, the change in the relation of the heat flux with the superheat is small with the variation of T_{sat}.

To obtain more spray cooling information, the effectiveness of spray cooling at CHF, η_c, SMD [8], d_{32}, and heat transfer coefficient of the spray cooling, h, are calculated. The effectiveness of spray cooling at CHF is defined as

$$\eta_c = \frac{q''_c}{h_{fg} Q'' \rho_l}. \tag{3}$$

The value of SMD is estimated using the following correlation [9]:

$$\frac{d_{32}}{d_0} = 3.07 \left(\frac{\rho_v^{0.5} \Delta p d_0^{1.5}}{\sigma^{0.5} \mu_l} \right)^{-0.259}. \tag{4}$$

The heat transfer coefficient of the spray cooling is defined as

$$h = \frac{q''}{T_w - T_{sat}}. \tag{5}$$

The maximum heat transfer coefficient obtained for a given saturation temperature is denoted by h_1. The results of η_c, d_{32} and h_1 as well as other five parameters for the four tested working fluids are listed in Table 1. It is shown that η_c is much smaller and d_{32} is greater for methanol than for FC-87 and FC-72 at the same Δp. Using the same multi-nozzle array, either methanol or water has the smallest η_c. The value of η_c decreases with Δp for FC-87 and FC-72 but increases slightly with Δp for methanol. Increasing Δp decreases d_{32} and generates more droplets. It is exhibited from the variations of h_1 with Δp that the spray heat transfer is enhanced with increasing the pressure drop. The highest heat transfer coefficient is obtained by using water as the working fluid. Since the subcooling of the working fluids is controlled to be as small as possible by using the preheater, the effect of the subcooling on the heat transfer coefficient and CHF is precluded from the discussion of the results.

As seen from Table 1, CHF increases with an increase of the volumetric flux or pressure drop. CHF increases with the saturation temperature in the present ranges of tested parameters. As shown in Table 1, the spray cooler can reach CHF of 90 W/cm^2 with FC-87

Table 1
Spray cooling parameters

Working fluid	T_b (°C)	T_{sat} (°C)	Δp (bar)	Q'' (m^3/m^2 s)	d_{32} (μm)	CHF (W/cm^2)	η_c	h_l (10^3 W/m^2 K)
FC-87	30	42.5	1.03	0.0147	45.3	79.0	0.374	15.8
			1.72	0.0181	39.6	87.5	0.336	19.5
			2.41	0.0204	36.5	90.0	0.306	20.6
FC-72	56	54	1.03	0.0144	52.1	65.0	0.324	16.7
			1.72	0.0175	45.2	72.5	0.300	19.4
			2.41	0.0201	41.4	78.5	0.282	20.7
			3.10	0.0222	38.7	83.5	0.271	22.3
Methanol	65	53	1.03	0.0246	79.6	357.5	0.122	46.8
			1.72	0.0308	68.6	440	0.131	57.2
			2.41	0.0363	62.3	490	0.133	64.5
Water	100	70	1.03	0.0188	111	>500	>0.116[a]	84.2
			1.72	0.0218	96.9	>500	>0.101[a]	94.6
			2.41	0.0249	88.8	>500	>0.088[a]	97.8

[a] At 500 W/cm^2.

fluids and 490 W/cm^2 with methanol. For water, the CHF is higher than 500 W/cm^2. CHF is caused by the inability of the liquid to reach the hot surface due to the entrainment of the countercurrent vapor flow in local regions and the splashing droplets. The mechanisms of CHF have been described [5–7]. Increasing Q'' enhances the momentum of the droplets and the capability of the droplets penetrating through the vapor flow to touch the hot surface.

5. Effect of noncondensible gas

The effect of noncondensible gas on the heat transfer of the spray cooling has not been addressed in literature. To discuss the effect of air on the thermal performance of the present spray cooling system, a spray cooling system with a certain amount of air is operated and compared with the system without air. In both cases, FC-72 is used as the working fluid. As the system is idling and not circulating, the spray chamber pressure is 0.85 bar for the system with the air and 0.295 bar for the system without air at the same room temperature of 25 °C. The relations of q'' with the hot surface temperature, T_w, for the cases with and without air in the system are plotted in Fig. 12. The spray chamber outlet temperature, $T_{ch,o}$, is used as a parameter (shown in Fig. 12) since it is difficult to determine the spray chamber saturation temperature if the system contains air which can be absorbed and released by FC-72 during its circulation in the closed loop. For comparison, the conditions of the cooling water supply from the cold bath are set to be the same in both systems with and without air involved. The liquid temperature at the inlet of the spray chamber is maintained at 30 °C. In the tested parameter ranges, the surface temperature is much lower for the system without air than for the system with the air for a given hot surface heat flux (below CHF). This is because the

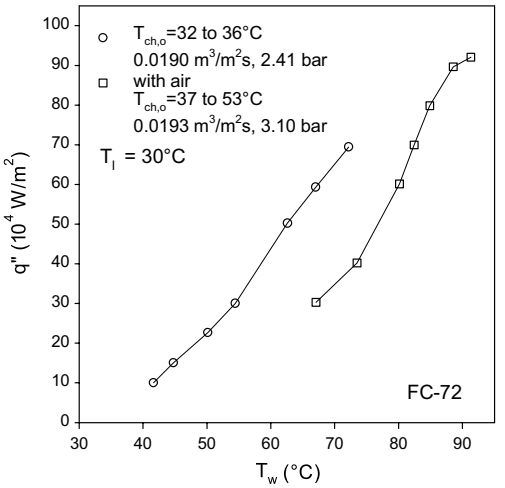

Fig. 12. Effect of noncondensible gas on the relation between heat flux and hot surface temperature.

noncondensible gas causes a higher system pressure, p_1, as shown in Fig. 3, and a higher spray chamber pressure which corresponds to a higher saturation temperature. The noncondensible gas increases an overall thermal resistance of the closed loop spray cooling system. It is believed that the noncondensible gas brings about a higher thermal resistance to the condensation heat transfer in the closed loop system. At 70 W/cm^2, the surface temperature is only 72.2 °C in the system with pure FC-72 while it is 82.4 °C in the system with the air.

Fig. 13 shows the effect of noncondensible gas on the heat transfer characteristics of the spray over the surface. The data points are plotted as q'' against $T_w - T_{ch,o}$. At the heat fluxes lower than 70 W/cm^2, the temperature difference of $T_w - T_{ch,o}$ is lower for the system without air than for the system with the air. This means that the system without air has a better thermal performance of

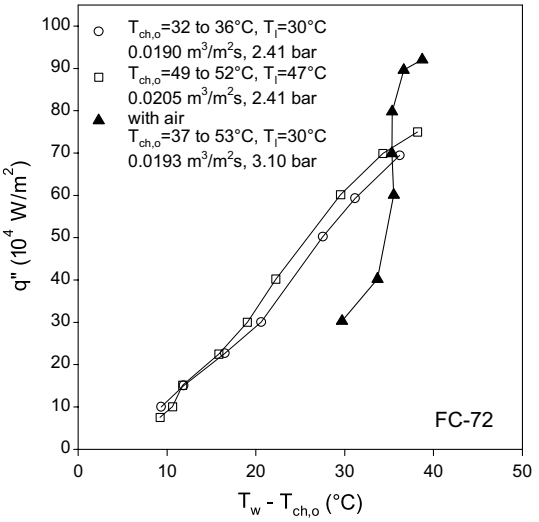

Fig. 13. Effect of noncondensible gas on heat transfer characteristics.

the spray over the surface at $q'' < 70$ W/cm^2. However, at $q'' > 70$ W/cm^2, the system with the air provides the smaller values of $T_w - T_{ch,o}$, showing a better thermal performance over the surface. This is due to the fact that FC-72 is sprayed along with the air that is released from FC-72 under a reduced pressure in the spray chamber. In this case, a thinner liquid film is produced on the cooling surface because the droplets are smaller in diameter and have higher velocities. Furthermore, the air flow field has increasing ability not only to spread the liquid film but also to replace the evaporating vapor and this results in a lower partial vapor pressure in the vicinity of the liquid film surface at the higher pressure drops. The secondary nucleation created by the air is more effective on the spray heat transfer over the hot surface than that by the vapor at the heat fluxes higher than 70 W/cm^2 in the case of FC-72.

6. Conclusions

1. A closed loop spray cooling test setup is established. A miniature nozzle array with eight miniature nozzles is designed that is capable of generating full cone sprays with spray cone angles larger than 35° at spray pressure drops greater than 1.72 bar.
2. The visual observation of the spray cooling in the confined chamber indicates that nucleate boiling heat transfer takes place in all tested cases and the other two heat transfer modes are convection heat transfer and evaporation from the surface of the liquid film. The interaction between the spray cone and surrounding fluid is stronger in the case of multi-nozzle spray cooling than in the case of single nozzle spray cooling.
3. FC-87, FC-72, methanol and water are used as the working fluids. Thermal performance data points for the multi-nozzle spray cooling in the confined and closed system are obtained at various operating temperatures, nozzle pressure drops (from 0.69 to 3.10 bar) and heat fluxes. For a given surface superheat, the heat flux increases with the volumetric flux. The pressure drop of 1.72 bar or lower are not optimum for the maximum heat removal.
4. The closed loop spray cooling can reach the CHF levels up to 90 W/cm^2 with pure FC-87, 490 W/cm^2 with pure methanol and greater than 500 W/cm^2 with pure water. CHF increases with an increase of the volumetric flux or pressure drop.
5. The noncondensible gas adversely affects the overall heat transfer of the closed loop spray cooling system at heat fluxes lower than CHF because of a higher thermal resistance to the condensation heat transfer. The system with pure FC-72 has a better thermal performance of the spray over the surface at $q'' < 70$ W/cm^2. However, at $q'' > 70$ W/cm^2, the system containing FC-72 and air shows a better thermal performance over the surface.

Acknowledgements

This research was supported by the Propulsion Directorate of the Air Force Research Laboratory (AFRL), Wright-Patterson Air Force Base, Ohio and performed at the Power Division's Thermal Laboratory. The authors wish to thank Richard J. Harris, University of Dayton Research Institute, for his efforts in designing and fabricating the nozzle array and establishing the data acquisition system. The authors also wish to thank John E. Tennant (UES, Inc.) for his support in machining and mounting the spray cooling system and Roger P. Carr for helping with data acquisition.

References

[1] J. Yang, L.C. Chow, M.R. Pais, Nucleate boiling heat transfer in spray cooling, J. Heat Transfer 118 (1996) 668–671.
[2] D.P. Rini, R.H. Chen, L.C. Chow, Bubble behavior and nucleate boiling heat transfer in saturated FC-72 spray cooling, J. Heat Transfer 124 (2002) 63–72.
[3] I. Mudawar, W.S. Valentine, Determination of the local quench curve for spray-cooled metallic surfaces, J. Heat Treating 7 (2) (1989) 107–121.
[4] M.S. Sehmbey, M.R. Pais, L.C. Chow, Effect of surface material properties and surface characteristics in evaporative

spray cooling, J. Thermophys. Heat Transfer 6 (3) (1992) 505–512.

[5] K.A. Estes, I. Mudawar, Correlations of Sauter mean diameter and critical heat flux for spray cooling of small surfaces, Int. J. Heat Mass Transfer 38 (16) (1995) 2985–2996.

[6] M.S. Sehmbey, L.C. Chow, O.J. Hahn, M.R. Pais, Effect of spray characteristics on spray cooling with liquid nitrogen, J. Thermophys. Heat Transfer 9 (4) (1995) 757–765.

[7] L. Lin, R. Ponnappan, Critical heat flux of multi-nozzle spray cooling in a closed loop, in: 37th Intersociety Energy Conversion Engineering Conference, Paper No. 20073, Washington, DC, 2002.

[8] A.H. Lefebvre, Atomization and Spray, Hemisphere, New York, 1989, pp. 105.

[9] I. Mudawar, K.A. Estes, Optimizing and predicting CHF in spray cooling of a square surface, J. Heat Transfer 118 (1996) 672–679.